Chemical Engineering Journal 123 (2006) 59–64

Chemical Engineering Journal

www.elsevier.com/locate/cej

Photocatalytic degradation of azo dye acid red G by KNb_3O_8 and the role of potassium in the photocatalysis

Gaoke Zhang *, Jie Gong, Xi Zou, Fangsheng He, Hao zhang,
Qiang Zhang, Ying Liu, Xia Yang, Bo Hu

School of Resources and Environmental Engineering, Wuhan University of Technology, 122 Luoshi Road, Wuhan 430070, People's Republic of China

Received 8 November 2005; received in revised form 25 April 2006; accepted 30 June 2006

Abstract

The layered photocatalyst KNb_3O_8 was prepared using a solid-state reaction method. Scanning electron microscope (SEM) and X-ray diffractometer (XRD) were used to characterize the photocatalyst. The photocatalytic degradation of acid red G over the photocatalyst under UV irradiation was studied. The influences of catalyst dosage, initial concentration of acid red G were determined as well. The kinetics of photocatalytic degradation of acid red G follows first-order kinetics. The H^+-exchanged KNb_3O_8 was prepared and its photocatalytic activity is much lower than that of the KNb_3O_8. The roles of the layered structure of the KNb_3O_8 and the potassium ions between the layers in the photocatalytic reaction were discussed.

Keyword: Photocatalysis; Photocatalytic degradation; Acid red G; Layered niobate; Potassium triniobate; Potassium

---

1. Introduction

In recent years, problem of wastewater became very important both for the sake of increasing amount and its variety. From the environment protection point of view, the textile industry is one of the special ones [1]. The wastewater of textile dye draining into the river without treatment will bring out serious pollution of water resource and threaten the ecology environment and human health [2]. Colored waters have a strong impact in the population and generate strong popular complaints [3]. Wastewaters from the textile industry are characterized mainly by high color resulting from considerable amounts of dyes [1]. The removal of organic pollutants in wastewater is an important measure in environmental protection. Dyestuffs and other commercial colorants have emerged as a focus of environmental remediation efforts [4].

A variety of physical, chemical and biological methods are presently available for treatment of textile wastewater. Biological treatment is a proven technology and is cost-effective. However, it has been reported that the majority of dyes are only adsorbed on the sludge and are not degraded. Physical methods are ion-exchange, adsorption, air stripping, etc. [5]. One difficulty with these methods is that they are not destructive but only transfer the contamination from one phase to another, therefore, a new and different kind of pollution is faced and further treatments are necessary [6]. Photocatalytic methods, using semiconductors, such as TiO_2, has attracted extensive attention, because they provide a promising strategy for cleaning polluted air or water [7]. Previous studies have shown that such semiconduction can degrade most kinds of persistent organic pollutant, such as dyes, pesticide, detergents and volatile organic compounds, under UV-light irradiation [7–10]. Owing to the semiconducting character of layered niobates such as $K_4Nb_6O_{17}$, some oxide derivatives have been used to achieve the water splitting to H_2 production by photocatalysis in the some studies [11]. Layered compounds, such as $K_4Nb_6O_{17}$ [12], Bi_2InNbO_7 [13], $Sr_2Nb_2O_7$ [14], Bi_2WO_4 [15], etc., have been attracting attention lately because they are much more active than the generally used TiO_2 or $SrTiO_3$ [16].

However, compared with other photocatalysts, the photocatalytic activity of niobate KNb_3O_8 for oxidizing organic contaminants in water has been less reported. KNb_3O_8 contains octahedral $[NbO_6]$ units forming an anionic sheet disposed in a stacking arrangement. The charge balance is maintained by the presence of potassium ions between the layers. In an earlier study, most of research works on KNb_3O_8 were focused on the

---

* Corresponding author. Tel.: +86 27 87887445; fax: +86 27 87887445.
E-mail address: gkzhang@mail.whut.edu.cn (G. Zhang).

1385-8947/$ – see front matter © 2006 Elsevier B.V. All rights reserved.
doi:10.1016/j.cej.2006.06.021

luminescence property of the compound [17–21]. In this article, the photocatalytic degradation of acid red G over KNb_3O_8 was examined. The role of potassium ions between the layers in the photocatalytic degradation of acid red G was study as well.

2. Experimental

2.1. Materials

The investigated acid red G (MW = 505 nm) was industrial dye and used without further purification. Other chemicals used in this experiment were analytical grade or chemical grade.

2.2. Preparation of KNb_3O_8 photocatalyst

Niobium pentoxide (Nb_2O_5) and potassium carbonate (K_2CO_3) were selected as starting materials for the preparation of KNb_3O_8. Before calcining, grinding the mixture adequately for 30 min was needed. KNb_3O_8 was prepared by solid-state reaction through heating a stoichiometic mixture of Nb_2O_5 and K_2CO_3 in Al_2O_3 crucible at 900 °C for 2 h. Considering the volatilization of potassium, 20% excessive potassium carbonate was added. After calcining, it was also necessary to grind the samples for 30 min again.

The calcined sample was washed with distilled water to remove the excess carbonate. Then the H^+-exchanged catalyst were obtained by suspending the prepared powder in a 5 mol/L HNO_3 at room temperature for 2 days under continuous stirring with the replacement of acid every 12 h.

2.3. Photocatalytic activity measurement

The degradation reaction of acid red G was carried out in a 500 mL Pyrex glass vessel with magnetic stirring at room temperature. Light source was a 20 W UV lamp ($\lambda = 253.7$ nm). Reaction suspension was prepared by adding a certain weight of prepared sample into a 150 mL of acid red G aqueous solution. Prior to irradiation, the suspensions were magnetically stirred without UV irradiation for 15 min to establish adsorption/degradation equilibrium. The distance between the liquid surface and the light source was about 8 cm. The light intensity was 0.750 mW/cm^2 measured by using an UV radiometer. The concentration of acid red G aqueous solution was determined by measuring the absorbance at 505 nm with an UV–vis spectrophotometer (UV-2100). Our experimental result showed that the linear relationship between the absorbance at 505 nm (A) and the acid red G (C) (mg/L) can be represented approximately by the equation:

$$A = 0.01C - 0.0003 \approx 0.01C \quad (2.1)$$

3. Result and discussion

3.1. Physical characterization of KNb_3O_8 photocatalyst

D/MAX-RB X-ray diffractometer (XRD, Rigaku, Japan) was used to record the KNb_3O_8 powder XRD patterns within a 2θ range from 5° to 70°. Fig. 1 shows the XRD pattern of the as-prepared KNb_3O_8 powder at 900 °C for 2 h. The XRD pattern can be identified and indexed using the standard XRD data for the KNb_3O_8. XRD peaks of KNb_3O_8 can nearly match up to the Standard XRD peaks, which shows the prepared sample consists of a nearly single phase of layered KNb_3O_8.

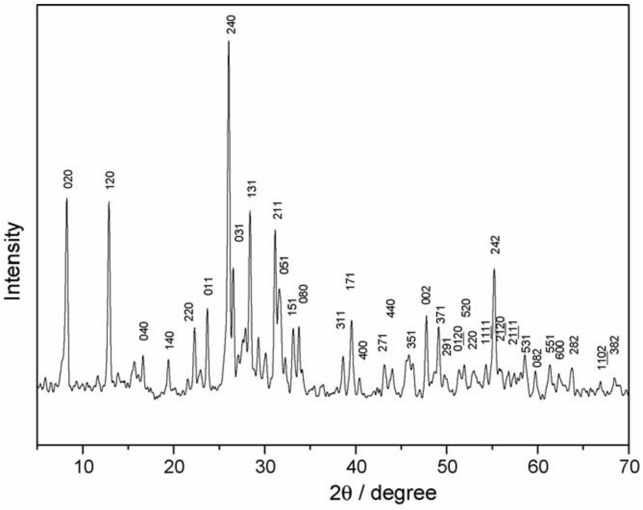

Fig. 1. Powder X-ray diffraction pattern of KNb_3O_8 synthesized at 900 °C for 2 h.

The crystal morphology of the as-prepared KNb_3O_8 powder was investigated by scanning electron microscopy (SEM). SEM was performed on JSM-5610 LV scanning electron microscope. As shown in Fig. 2, the average size of KNb_3O_8 crystal particles was estimated to be around 1.5 μm. The SEM photograph shows that the size of potassium triniobate particle is more uniform.

3.2. Photocatalytic activity of KNb_3O_8 photocatalyst

3.2.1. Comparative experiments

In order to confirm the photocatalytic activity of KNb_3O_8 for the degradation of acid red G under UV light, a series of comparative experiments were carried out through using the

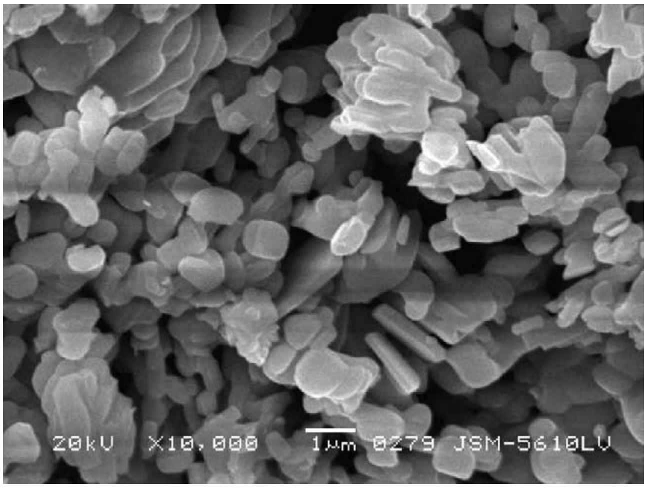

Fig. 2. SEM image of KNb_3O_8 powder.

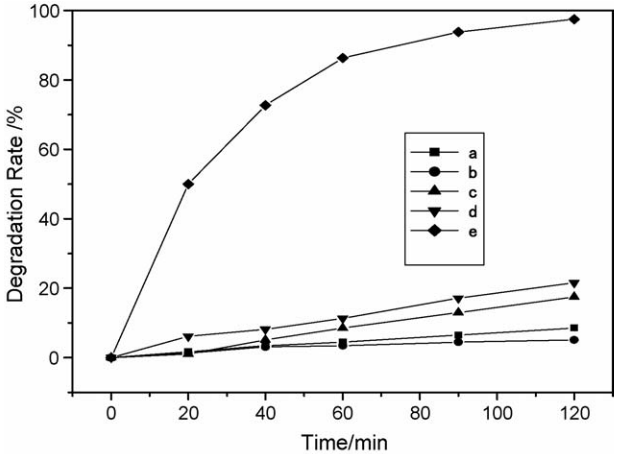

Fig. 3. The degradation rate of acid red G at different experimental conditions: (a) under UV light in the absence of KNb_3O_8; (b) KNb_3O_8 catalyst in the dark; (c) the same weight Nb_2O_5 instead of KNb_3O_8 under UV irradiation; (d) the same weight stoichiometic mixture of Nb_2O_5 and K_2CO_3 instead of KNb_3O_8 under UV light; (e) KNb_3O_8 under UV light.

starting material Nb_2O_5 or the stoichiometic mixture of Nb_2O_5 and K_2CO_3 instead of KNb_3O_8 or in the absence of KNb_3O_8 under UV light and in the presence of KNb_3O_8 catalyst in the dark. The experiments were evaluated by the photocatalytic degradation of 30 mg/L concentration acid red G. The catalyst dosage was 1.0 g/L. Fig. 3 shows the result of comparative experiments. The degradation rates of acid red G are very low and negligible within the time of these experiments except when using KNb_3O_8 catalyst under UV irradiation, which illustrates that the observed degradation of acid red G is attributed to the photocatalytic effect of KNb_3O_8 under UV irradiation. This is neither the direct photodegradation of acid red G by UV light, the photocatalytic degradation of acid red G by the starting material Nb_2O_5, nor the mixture of Nb_2O_5 and K_2CO_3 under UV irradiation.

3.2.2. Photocatalytic degradation of acid red G at different concentration by KNb_3O_8

The degradation of acid red G at different concentrations by KNb_3O_8 was studied as well. The dosage of KNb_3O_8 was 1.0 g/L. As it is shown in Fig. 4, although the degradation rate of acid red G decreases with increasing of its initial concentration, the decreases are smaller. The photocatalytic degradation rate of 10 mg/L acid red G by KNb_3O_8 reached 100% under UV irradiation for 60 min. After 120 min under UV irradiation, 97.6 and 85.5% degradation rate could be reached when the initial concentration of acid red G was 20 and 60 mg/L, respectively.

3.2.3. Effect of catalyst dosage

It can be seen that the concentration of KNb_3O_8 catalyst has a great effect on the decomposition rate of acid red G from Fig. 5. The degradation rate of 30 mg/L acid red G increases with increasing of the catalyst dosage. When the catalyst KNb_3O_8 concentration was about 0.3 and 0.6 g/L, the degradation rate of acid red G under UV irradiation for 120 min was about 81.6 and 97.22%, respectively. When the catalyst concentration reached 2.0 g/L, the degradation rate was 100%, which means the complete degradation of acid red G.

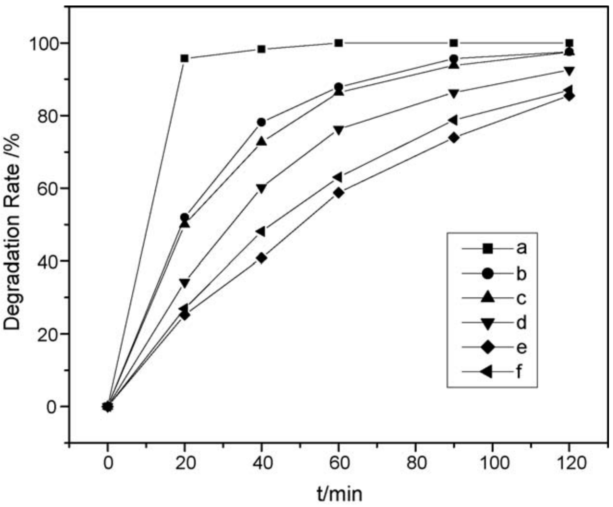

Fig. 4. The photocatalytic degradation rate of acid red G at different concentration: (a) 10 mg/L; (b) 20 mg/L; (c) 30 mg/L; (d) 40 mg/L; (e) 50 mg/L; (f) 60 mg/L.

3.2.4. Kinetics of photocatalytic degradation of acid red G by KNb_3O_8

The photocatalytic degradation of many dyes always follows Langmiur–Hinshelwood kinetics model (L-H model) [22–25], which is described as Eq. (3.1):

$$r = -\frac{dC}{dt} = \frac{kKC}{1 + KC} \tag{3.1}$$

where r is reaction velocity, C the dye concentration, and k and K are the surface reaction velocity and adsorption constant, respectively. Clearly, the adsorption of dye on the catalyst is not saturated and $KC \ll 1$ when the dye concentration is very low,

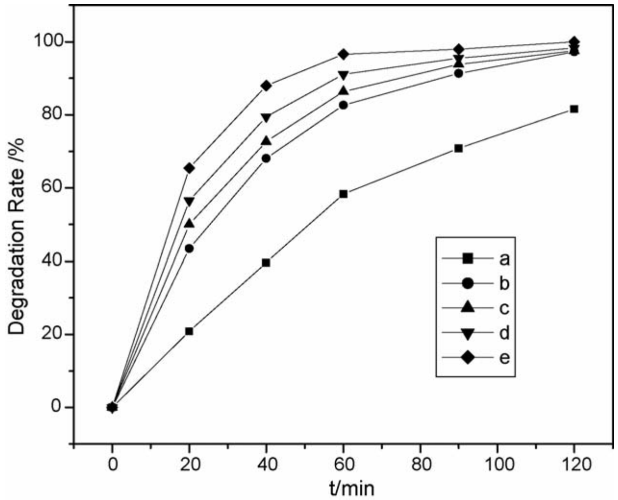

Fig. 5. The degradation rates of acid red G by KNb_3O_8 with different dosages: (a) 0.3 g/L; (b) 0.6 g/L; (c) 1.0 g/L; (d) 1.5 g/L; (e) 2.0 g/L.

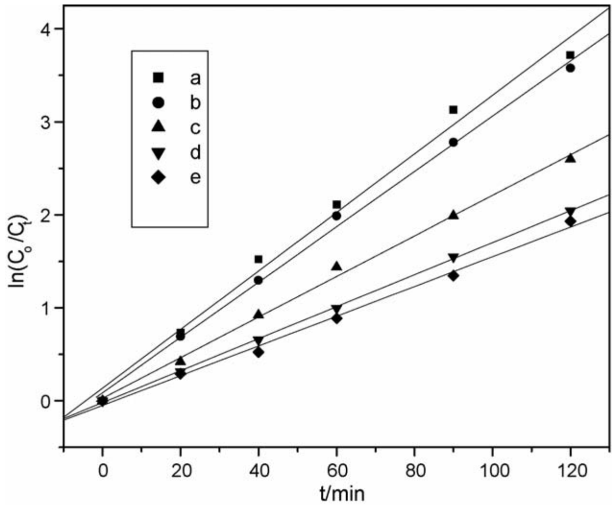

Fig. 6. Relationship between $\ln(C_0/C_t)$ and treatment time. Initial concentration of acid red G: (a) 20 mg/L; (b) 30 mg/L; (c) 40 mg/L; (d) 50 mg/L; (e) 60 mg/L.

the L-H model can be described as Eq. (3.2):

$$\ln\left(\frac{C_0}{C_t}\right) = k\,(\text{min}^{-1})t + a \tag{3.2}$$

where C_0 is the initial concentration of dye and k is the apparent reaction rate. The relation between $\ln(C_0/C_t)$ and t is linear. The $\ln(C_0/C_t)$ of acid red G is equal to its $\ln(A_0/A_t)$ according to the linear Eq. (2.1). Fig. 6 shows the fitted plots of $\ln(C_0/C_t)$ as a function of UV irradiation time at different acid red G concentrations. From the results, there is very well linear relation between $\ln(C_0/C_t)$ and t for the photocatalytic degradation of acid red G by KNb_3O_8 and the kinetics of the photodegradation reaction follows first-order reaction. Parameters and first-order reaction kinetic equations for different initial acid red G concentrations are given in Table 1. It can be seen that the apparent reaction rate constant k deceases with increasing of the acid red G initial concentration.

3.2.5. UV–vis absorption spectra

Absorption spectra recorded during the photodegradation of acid red G by KNb_3O_8 are given in Fig. 7, and the initial concentration of acid red G was 30 mg/L. From the results, the characteristic absorption peaks of acid red G decreased with increasing of irradiation time, and finally disappeared and the acid solution became colorless. The acid red G is with three characteristic peaks in ultraviolet band. The peak at 215 nm is attributed to the structure of benzene ring, and the peak around 330 nm is related to the structure of naphthalene ring. The third peak at 505 nm is the characteristic peak of acid red G. The intensity of the peak at 505 nm decreased with increasing of irradiation time, which means the chromophoric unsaturated conjugated bond in the dye molecule was destroyed gradually. The peak at 505 nm nearly disappeared after 60 min, and the peak of benzene ring and naphthalene ring also disappeared gradually. These results indicate that photocatalytic degradation not only destroys the conjugate system (including –N=N–), but also partly decomposes the benzene and naphthalene rings in molecule.

Table 1
Parameters and first-order reaction kinetic equations for different initial concentrations

C_0 (mg/L)	First-order reaction kinetic equation	k	R
20	$\ln(C_0/C_t) = 0.03149t + 0.13658$	0.03149	0.9934
30	$\ln(C_0/C_t) = 0.02975t + 0.08653$	0.02975	0.99838
40	$\ln(C_0/C_t) = 0.02184t + 0.02705$	0.02184	0.99836
50	$\ln(C_0/C_t) = 0.01721t - 0.0198$	0.01721	0.99976
60	$\ln(C_0/C_t) = 0.01598t - 0.049$	0.01598	0.99739

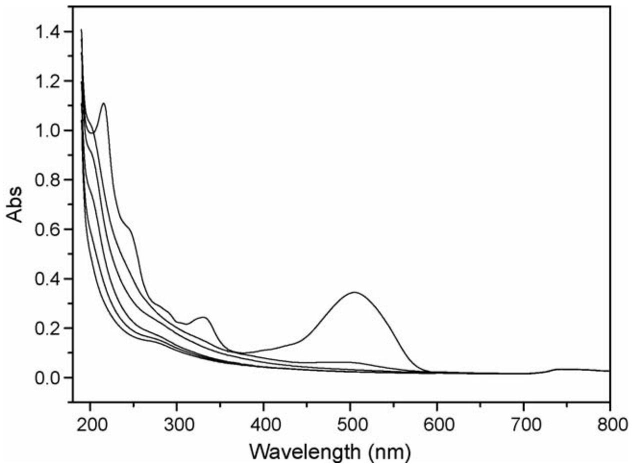

Fig. 7. UV–vis spectra changes during photocatalytic degradation of 30 mg/L acid red G by KNb_3O_8 at reaction time of 0, 20, 40, 60, 90 and 120 min, respectively.

The color of azo dyes is determined according to the azo bonds and their associated chromophores and auxochromes [26]. Azo bands are the most active bonds in azo dye molecules, which are liable to be oxidized by positive hole or hydroxyl radical or reduced by electron in the conduction band [27–29]. The reaction of azo bands lead to the decoloration of dyes.

3.3. The role of the potassium ions in the layered structure of the KNb_3O_8

Fig. 8 shows the photocatalytic degradation of 20 mg/L acid red G under UV irradiation over the H^+-exchanged. The catalyst dosage was 1.0 g/L. As a comparison, the photodegradation of the 20 mg/L acid red G over the KNb_3O_8 was given too. Usually, protonation can enhance the photocatalytic activity of catalyst. Shimizu et al. found that the layered perovskite tantalate with hydrated interlayer space, $H_2SrTa_2O_7{\cdot}nH_2O$ shows higher H_2 formation rate than anhydrous layered tantalate $Li_2SrTa_2O_7$ and high activity for overall splitting of water without loading co-catalysts. The reaction over $H_2SrTa_2O_7{\cdot}nH_2O$ proceeded steadily more than 70 h, demonstrating a high durability of the catalyst [30]. Kudo et al. studied the photocatalytic activities of triple-layered Aurivillius phases, $Bi_2A'NaNb_3O_{12}$ (A' = Sr, Ca) and $Bi_2CaNaTa_3O_{12}$, and of protonated forms prepared from these Aurivillius phases through selective leaching of bismuth oxide sheets. The result showed that all the corresponding protonated forms show photocatalytic activities for H_2 evolution

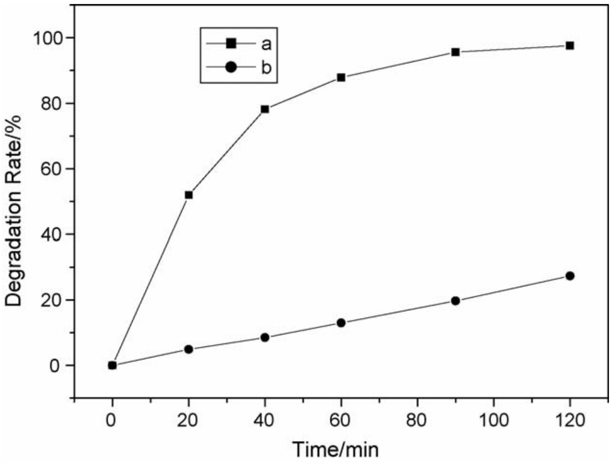

Fig. 8. The photodegradation of 20 mg/L acid red G over KNb_3O_8 (a) and the H^+-exchanged KNb_3O_8 (b), respectively.

[31]. However, our result on the photodegradation of acid G over KNb_3O_8 shows that the degradation rate of acid red G over the H^+-exchanged KNb_3O_8 under UV irradiating for 120 min is only 27.35%, which is much lower than the 97.57% degradation rate of acid red G over the KNb_3O_8 markedly.

The structure of the KNb_3O_8 is very important for photodegradating the acid red G. The KNb_3O_8 is a kind of perovskite-type compound with layered structure. The layered materials use their interlayer space as reaction sites for water splitting, where electron–hole recombination process could be retarded by physical separation of electron and hole pairs generated by photoabsorption. These high activities resulted from their layered structure and the high concentration of donor level compared with bulk-type perovskite photocatalysts [30,32,33]. The photocatalytic activity of the layered compound is sensitive to its interlayer cations [34]. Morawski et al. [35] found that the photocatalytic activity of pure TiO_2 is much lower than K–TiO_2 in the photoreaction of phenol decomposition. They thought that the layered perovskite structure of the $K_2Ti_4O_9$ in the K–TiO_2 offers the possibility of decomposition of phenol and products of phenol. The presence of potassium in the K–TiO_2 material probably accelerates the electron–hole creation. The efficiency of K-modified titanium dioxide nanoparticles, which were prepared by impregnation, is better than that of TiO_2-P25 and the doped-TiO_2 can be considered as promising materials for organic pollutants degradation [36]. Electro-pumping of *K* to the surfaces of metal catalyst films can lead to very large and reversible changes in catalytic activity. Potassium-containing vanadium catalysts revealed significant higher performance compared to vanadium phosphate solids [37]. The alkali added to the Cu-Na-ZSM-5 zeolite was thus found to selectively promote catalytic activity for the partial oxidation of benzyl alcohol and prevent the deactivation of the Cu-Na-ZSM-5 zeolite [38]. Zhu and Lu [39] investigated catalytic conversion of N_2O to N_2 with potassium catalysts supported on activated carbon (K/AC). Their results showed that potassium is much more active and stable than either copper or cobalt, and the catalytic role of potassium is also attributed to its effective participation in an oxidation–reduction (redox) cycle. The excellent activity of K/AC catalysts indicates that not only is the potassium catalyst an easy acceptor of oxygen but it also possesses a strong ability for oxygen transfer. Shangguan et al. [40] proved that potassium is the most effective dopant and the most popular promoter to $CuFe_2O_4$. Potassium was found to be the most effective additive for Co_3O_4 catalysts and the addition of potassium increased not only the surface area but also the specific activity per unit surface area as well [41]. The TiO_2/KOH photocatalyst appeared to be more active in the reaction of photocatalytic decomposition of oil than TiO_2 [42]. In fact, Owing to their exceptionally low ionization potentials, alkali metals can act as electronic promoters modifying simultaneously the acid–base function of the surface. From our results, the photocatalytic efficiency of the KNb_3O_8 is much higher than that of the H^+-exchanged KNb_3O_8. In the processes of photodegradating acid red G, the holes created by the catalyst under UV irradiation can react with OH^- or H_2O to form $^\bullet OH$ radicals which can also oxidize the dye, while photogenerated electron can react with the pre-adsorbed oxygen [29]. Firstly, the interlayer spaces of the KNb_3O_8 promote the generation and the separation of the charge carriers and are beneficial to the transfer of electrons to the surface of the photocatalyst along the layered network, where electron–hole recombination process could be retarded by physical separation of electron and hole pairs generated by photoabsorption [30,32,33,43]. Secondly, potassium ions between the perovskite layers of the KNb_3O_8 are effective electronic promoter and accelerate the electron–hole creation. Thirdly, potassium is not only an easy acceptor of oxygen but it also possesses a strong ability for oxygen transfer. So, potassium ions can increase the photocatalytic activity of the KNb_3O_8 largely.

4. Conclusion

The layered perovskite KNb_3O_8 was prepared by a solid-state reaction method. The degradation rate of acid red G decreases with increasing of acid red G concentration and increases with increasing of the catalyst dosage. The kinetics of photocatalytic degradation of acid red G follows first-order kinetics equation. The photocatalytic efficiency of the KNb_3O_8 is much higher than that of the H^+-exchanged KNb_3O_8. The layered structure of the KNb_3O_8 and the potassium ions between the layers play an important role on the photocatalytic degradation of acid red G.

Acknowledgement

This work was supported by the Natural Science Foundation of China (50472017).

References

[1] B. Zielińska, J. Grzechulska, R.J. Kaleńczuk, A.W. Morawski, The pH influence on photocatalytic decomposition of organic dyes over A11 and P25 titanium dioxide, Appl. Catal. B: Environ. 45 (2003) 293–300.

[2] M.Q. Hu, Y.M. Xu, Photocatalytic degradation of textile dye X3B by heteropolyoxometalate acids, Chemosphere 54 (2004) 431–434.

[3] C.G. da Silva, J.L. Faria, Photochemical and photocatalytic degradation of an azo dye in aqueous solution by UV irradiation, J. Photochem. Photobiol. A: Chem. 155 (2003) 133–143.

[4] S. Sakthivela, B. Neppolianb, M.V. Shankarb, B. Arabindoo, M. Palanichamyb, V. Murugesanb, Solar photocatalytic degradation of azo dye: comparison of photocatalytic efficiency of ZnO and TiO_2, Solar Energy Mater. Solar Cells 77 (2003) 65–82.

[5] T. Sauer, G.C. Neto, H.J. José, R.F.P.M. Moreira, Kinetics of photocatalytic degradation of reactive dyes in a TiO_2 slurry reactor, J. Photochem. Photobiol. A: Chem. 149 (2002) 147–154.

[6] N. Daneshvar, D. Salari, A.R. Khataee, Photocatalytic degradation of azo dye acid red 14 in water: investigation of the effect of operational parameters, J. Photochem. Photobiol. A: Chem. 157 (2003) 111–116.

[7] M.R. Hoffmann, S.T. Martin, W.Y. Choi, D.W. Bahnemann, Environmental applications of semiconductor photocatalysis, Chem. Rev. 95 (1995) 69–96.

[8] C. Wang, J. Zhao, X. Wang, B. Mai, G. Sheng, P. Peng, J. Fu, Preparation, characterization and photocatalytic activity of nano-sized ZnO/SnO_2 coupled photocatalysts, Appl. Catal. B: Environ. 39 (2002) 269–279.

[9] A.L. Linsebigler, G.Q. Lu, J.T. Yates Jr., Photocatalysis on TiO_2 surfaces: principles, mechanisms, and selected results, Chem. Rev. 95 (1995) 735–758.

[10] T. Torimoto, S. Ito, S. Kuwabate, H. Yoneyama, Effects of adsorbents used as supports for titanium dioxide loading on photocatalytic degradation of propyzamide, Environ. Sci. Technol. 30 (1996) 1275–1281.

[11] K. Sayama, A. Tanaka, K. Domen, K. Marnya, T. Photocatalytic decomposition of water over platinum-intercalated potassium niobate ($K_4Nb_6O_{17}$), Onishi, J. Phys. Chem. 95 (1991) 1345–1348.

[12] S. Uchida, Y. Fujishiro, A. Watanabe, O. Ito, T. Sato, Intercalation of titanium oxide in layered $H_2Ti_4O_9$ and $H_4Nb_6O_{17}$ and photocatalytic water cleavage with $H_2Ti_4O_9/(TiO_2, Pt)$ and $H_4Nb_6O_{17}/(TiO_2, Pt)$ nanocomposites, J. Chem. Soc. Dalton Trans. 93 (1997) 3229–3234.

[13] Z. Zou, J.H. Ye, H. Arakawa, Substitution effects on In^{3+} by Al^{3+} and Ga^{3+} on the photocatalytic and structural properties of the Bi_2InNbO_7 photocatalyst, Chem. Mater. 13 (2001) 1765–1769.

[14] G.K. Hyun, W.H. Dong, K. Jindo, G.K. Young, S.L. Jae, Highly donor-doped (1 1 0) layered perovskite materials as novel photocatalysts for overall water splitting, Chem. Commun. (1999) 1077–1078.

[15] J.G. Yu, J.F. Xiong, B. Cheng, Y. Yu, J.B. Wang, Hydrothermal preparation and visible-light photocatalytic activity of Bi_2WO_6 powders, J. Solid State Chem. 178 (2005) 1968–1972.

[16] W.F. Yao, H. Wang, X.H. Xu, S.X. Shang, Y. Hou, Y. Zhang, M. Wang, Synthesis and photocatalytic property of bismuth titanate $Bi_4Ti_3O_{12}$, Mater. Lett. 57 (2003) 1899–1902.

[17] G. Blasse, F. van Tol, Luminescence of KNb_3O_8, Solid State Commun. 95 (1995) 465–468.

[18] V.R.L. Constantino, M.A. Bizeto, H.F. Brito, Photoluminescence study of layered niobates intercalated with Eu^{3+} ions, J. Alloys Compd. 278 (1998) 142–148.

[19] A. Kudo, E. Kaneko, Photoluminescent properties of ion-exchangeable layered oxides, Microporous Mesoporous Mater. 21 (1998) 615–620.

[20] M. Gasperin, Strcture du trinibqte (V) de potqssium KNb_3O_8 un niobate lamellaire, Acta Cryst. B 38 (1982) 2024–2026.

[21] M.A. Bizeto, D.L.A. de Faria, V.R.L. Constantino, Organic–inorganic hybrid material synthesized by porphyrin intercalation into a layered niobate host matrix, J. Mater. Sci. Lett. 18 (1999) 643–646.

[22] D.F. Ollis, Contaminant degradation in water: heterogeneous photocatalysis degrades halogenated hydrocarbon contaminants, Environ. Sci. Technol. 19 (1985) 480–484.

[23] R.W. Matthews, Photooxidation of organic impurities in water using thin films of titanium dioxide, J. Phys. Chem. 91 (1987) 3328–3333.

[24] C.S. Turchi, D.F. Ollis, Photocatalytic degradation of organic water contaminants: mechanism involving hydroxyl radical attack, J. Catal. 122 (1990) 178–192.

[25] A. Mills, R.H. Davies, D. Worsley, Water purification by semiconductor photocatalysis, Chem. Soc. Rev. 27 (1993) 417–425.

[26] B. Reutergardh, L.M. Iangphasuk, Photocatalytic decolourization of reactive azo dye: a comparison between TiO_2 and us photocatalysis, Chemosphere 35 (1997) 585–596.

[27] R. Ganesh, G.D. Boardman, D. Michelssen, Fate of azo dyes in sludges, Water Res. 28 (1994) 1367–1376.

[28] H. Hidaka, J. Zhao, E. Pelizzatti, N. Serpone, Photodegradation of surfactants. 8. Comparison of photocatalytic processes between anionic DBS and cationic BDDAC on the titania surface, J. Phys. Chem. 96 (1992) 2226–2230.

[29] J.G. Yu, X.J. Zhao, Q.N. Zhao, Effect of surface structure on photocatalytic activity of TiO_2 thin films prepared by sol–gel method, Thin Solid Films 379 (2000) 7–14.

[30] K. Shimizu, Y. Tsuji, T. Hatamachi, K. Toda, T. Kodama, M. Sato, Y. Kitayama, Photocatalytic water splitting on hydrated layered perovskite tantalate $A_2SrTa_2O_7{\cdot}nH_2O$ (A = H, K, and Rb), Phys. Chem. Chem. Phys. 6 (2004) 1064–1069.

[31] M. Kudo, S. Tsuzuki, K. Katsumata, A. Yasumori, Y. Sugahara, Effects of selective leaching of bismuth oxide sheets in triple-layered Aurivillius phases on their photocatalytic activities, Chem. Phys. Lett. 393 (2004) 12–16.

[32] D.W. Hwang, H.G. Kim, J. Kim, K.Y. Cha, Y.G. Kim, J.S. Lee, Photocatalytic water splitting over highly donor-doped (1 1 0) layered perovskites, J. Catal. 193 (2000) 40–48.

[33] T. Takata, K. Shinohara, A. Tanaka, M. Hara, J.N. Kondo, K. Domen, A highly active photocatalyst for overall water splitting with a hydrated layered perovskite structure, J. Photochem. Photobiol. A: Chem. 106 (1997) 45–49.

[34] M. Machida, K. Miyazaki, S. Matsushima, M. Arai, Photocatalytic properties of layered perovskite tantalates, $MLnTa_2O_7$ (M = Cs, Rb, Na, and H; Ln = La, Pr, Nd, and Sm), J. Mater. Chem. (2003) 1433–1437.

[35] A.W. Morawski, J. Grzechulska, K. Kalucki, A new method for preparation of potassium-pillared layered titanate applied in photocatalysis, J. Phys. Chem. Solids 57 (1996) 1011–1017.

[36] Y. Bessekhouad, D. Robert, J.V. Weber, N. Chaoui, Effect of alkaline-doped TiO_2 on photocatalytic efficiency, J. Photochem. Photobiol. A: Chem. 167 (2004) 49–57.

[37] A. Martin, U. Bentrup, G.U. Wolf, The effect of alkali metal promotion on vanadium-containing catalysts in the vapour phase oxidation of methyl aromatics to the corresponding aldehydes, Appl. Catal. A: Gen. 227 (2002) 131–142.

[38] H. Hayashibara, S. Nishiyarna, S. Tsuruya, M. Masai, The effect of alkali promoters on Cu-Na-ZSM-5 catalysts in the oxidation of benzyl alcohol, J. Catal. 153 (1995) 254–264.

[39] Z.H. Zhu, G.Q. Lu, Catalytic conversion of N_2O to N_2 over potassium catalyst supported on activated carbon, J. Catal. 187 (1999) 262–274.

[40] W.F. Shangguan, Y. Teraoka, S. Kagawa, Promotion effect of potassium on the catalytic property of $CuFe_2O_4$ for the simultaneous removal of NO_x and diesel soot particulate, Appl. Catal. B: Environ. 16 (1998) 149–154.

[41] M. Haneda, Y. Kintaichi, N. Bion, H. Hamada, Alkali metal-doped cobalt oxide catalysts for NO decomposition, Appl. Catal. B: Environ. 46 (2003) 473–482.

[42] J. Grzechulska, M. Hamerski, A.W. Morawski, Photocatalytic decomposition of oil in water, Water Res. 34 (2000) 1638–1644.

[43] J. Tang, Z. Zou, J. Ye, Physical and photocatalytic properties of $AgInW_2O_8$, J. Phys. Chem. B 107 (2003) 14265–14269.